On the Sensitivity of Measured Backscattering Properties to Variations of Incidence Angle and Baselines in Tomographic SAR Data

Othmar Frey
Earth Observation & Remote Sensing
ETH Zurich, Switzerland /
Gamma Remote Sensing,
Switzerland
Email: otfrey@ethz.ch

Erich Meier
Remote Sensing Laboratories
University of Zurich
Switzerland

Irena Hajnsek
Earth Observation & Remote Sensing
ETH Zurich, Switzerland /
German Aerospace Center - DLR,
Germany

***Abstract*—SAR tomography at L- and P-bands reveals 3-D structural information of forested areas. A drawback, however, are the large number of samples, i.e. overflights, typically used for such configurations. Based on two fully-polarimetric tomographic SAR data sets, at L- and P-bands, we analyze the sensitivity of backscattering from a forest volume as measured by means of SAR tomography with respect to (1) a reduction of the total baseline by subsequently reducing the number of baselines, and (2), with respect to a variation of the incidence angle. In this paper, an excerpt of this sensitivity analysis is presented and discussed.**

I. Introduction

The benefit of SAR tomography concepts for imaging of vegetation volumes of forested areas, which are semitransparent to microwaves in the decimeter to meter range, was demonstrated in a number of experiments and using different processing approaches over the recent years [1]–[13]. In view of more operational data acquisition scenarios the number of baselines should be reduced [7] and, thus, a baseline configuration that is optimal with respect to the mission's purpose is to be envisioned. Examples include the extraction of a digital elevation model below forest canopy, on the one hand, and the extraction of vegetation height and further vegetation parameters by means of a polarimetric or a combined polarimetric-interferometric processing and analysis of the SAR tomography data, on the other hand. Recently, we have analyzed the focusing performance of different tomographic focusing techniques [12] using the full synthetic aperture (SA) and a reduced synthetic aperture in the normal direction (i.e., the direction perpendicular to line of sight). In addition, the resulting three-dimensional data cubes obtained from time-domain SAR tomography were analyzed with respect to the frequencies L-band and P-band, the polarization, and three focusing techniques in [13].

Using the same multibaseline SAR data sets, we have now extended our data analysis by looking at potential sensitivities of the measured backscattering values of a forest at L- and P-bands as a function of total baseline length and location of the respective subapertures, or equivalently, a variation of the mean incidence angle. To this end, a number of different tomographic subapertures of both data sets were processed.

TABLE I
E-SAR system specifications and nominal parameters of the tomographic acquisition patterns for both multibaseline data sets at P-band and L-band.

	P-band	**L-band**
Carrier frequency	350 MHz	1.3 GHz
Chirp bandwidth	70 MHz	94 MHz
Sampling rate	100 MHz	100 MHz
PRF	500 Hz	400 Hz
Ground speed	90 m/s	90 m/s
No. of data tracks	11+1	16+1
Nominal track spacing d_n	57 m	14 m
Horizontal baselines	40 m	10 m
Vertical baselines	40 m	10 m
Synthetic aperture in normal direction L	570 m	210 m
Nominal resolution in normal direction δ_n	3 m	2 m
Approx. unambiguous height H	30 m	30 m

In this paper, we present an excerpt of this ongoing analysis of two airborne tomography data sets at L- and P-bands (see Table I) of a forested area located in Switzerland. The sensitivity of the measured backscattering location and intensity to variations of the total number of flight tracks (FT) and different selections of subsets of baselines —and therefore also different incidence angles—is assessed by means of vertical plots of intensities obtained from tomographically focusing the data using different subapertures in the normal direction.

In the following, a selection of the resulting vertical profiles of intensities are presented and discussed.

II. Methods and Data

The analysis is based on two fully polarimetric airborne multibaseline data sets, at L- and P-bands, recently described in detail in [13]. A description of the data processing and

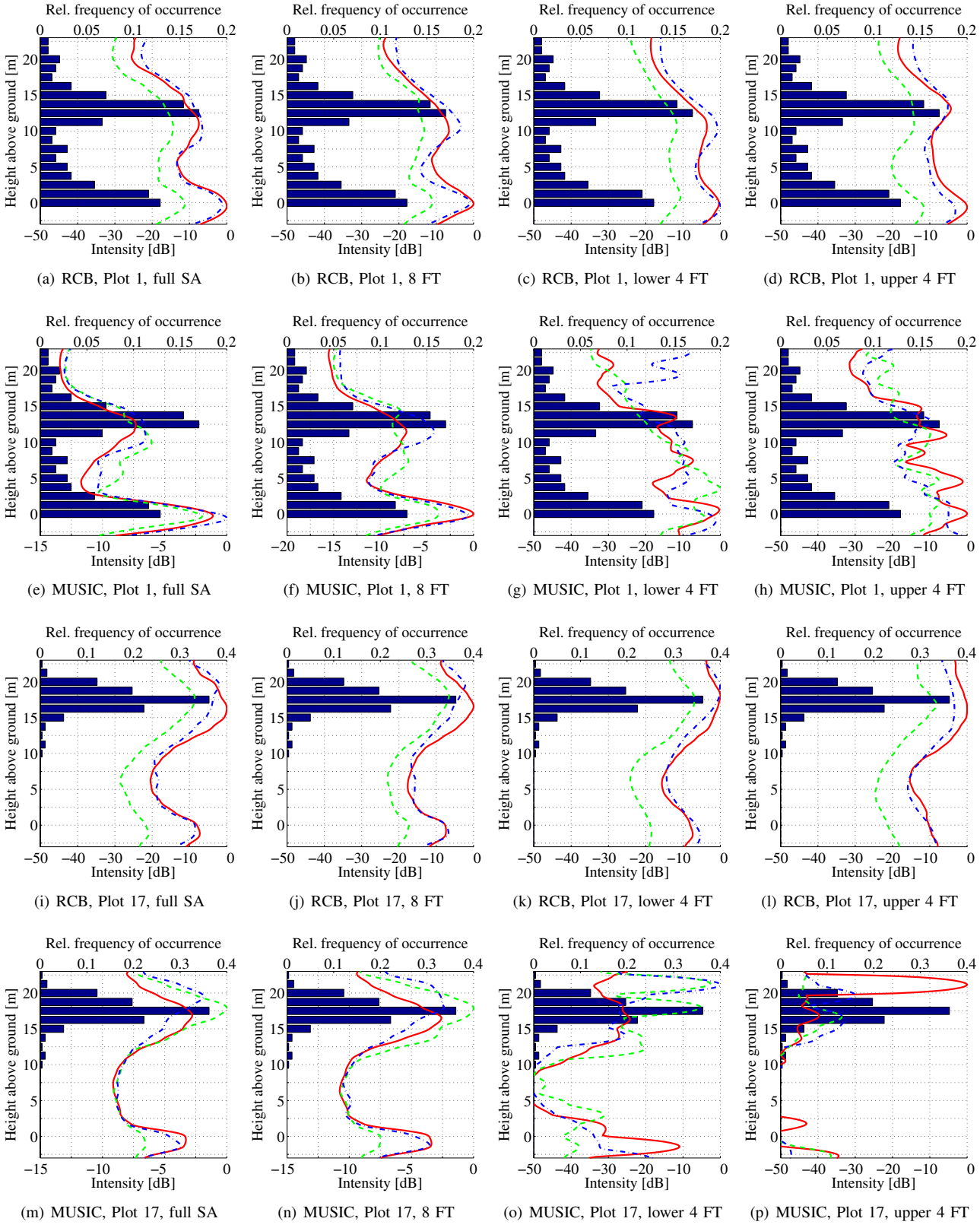

(a) RCB, Plot 1, full SA (b) RCB, Plot 1, 8 FT (c) RCB, Plot 1, lower 4 FT (d) RCB, Plot 1, upper 4 FT

(e) MUSIC, Plot 1, full SA (f) MUSIC, Plot 1, 8 FT (g) MUSIC, Plot 1, lower 4 FT (h) MUSIC, Plot 1, upper 4 FT

(i) RCB, Plot 17, full SA (j) RCB, Plot 17, 8 FT (k) RCB, Plot 17, lower 4 FT (l) RCB, Plot 17, upper 4 FT

(m) MUSIC, Plot 17, full SA (n) MUSIC, Plot 17, 8 FT (o) MUSIC, Plot 17, lower 4 FT (p) MUSIC, Plot 17, upper 4 FT

Fig. 1. Vertical profiles of relative intensities from L-band tomographic data of a forest (Plot 1 and 17) averaged over a circular sample plot of 300m^2 for the polarimetric channels HH (—), HV (– –), and VV (·–), RCB, and MUSIC. In each row, the following sequence of number of flight tracks (FT) is given, from left to right: (1) full SA (16 FT), (2) approx. half the SA (8 FT), (3) the lower 4 flight tracks, and (4) the upper 4 flight tracks. For comparison, histograms of height differences between the ALS DSM and the ALS DEM are underlaid as an external estimate of the distribution of tree heights.

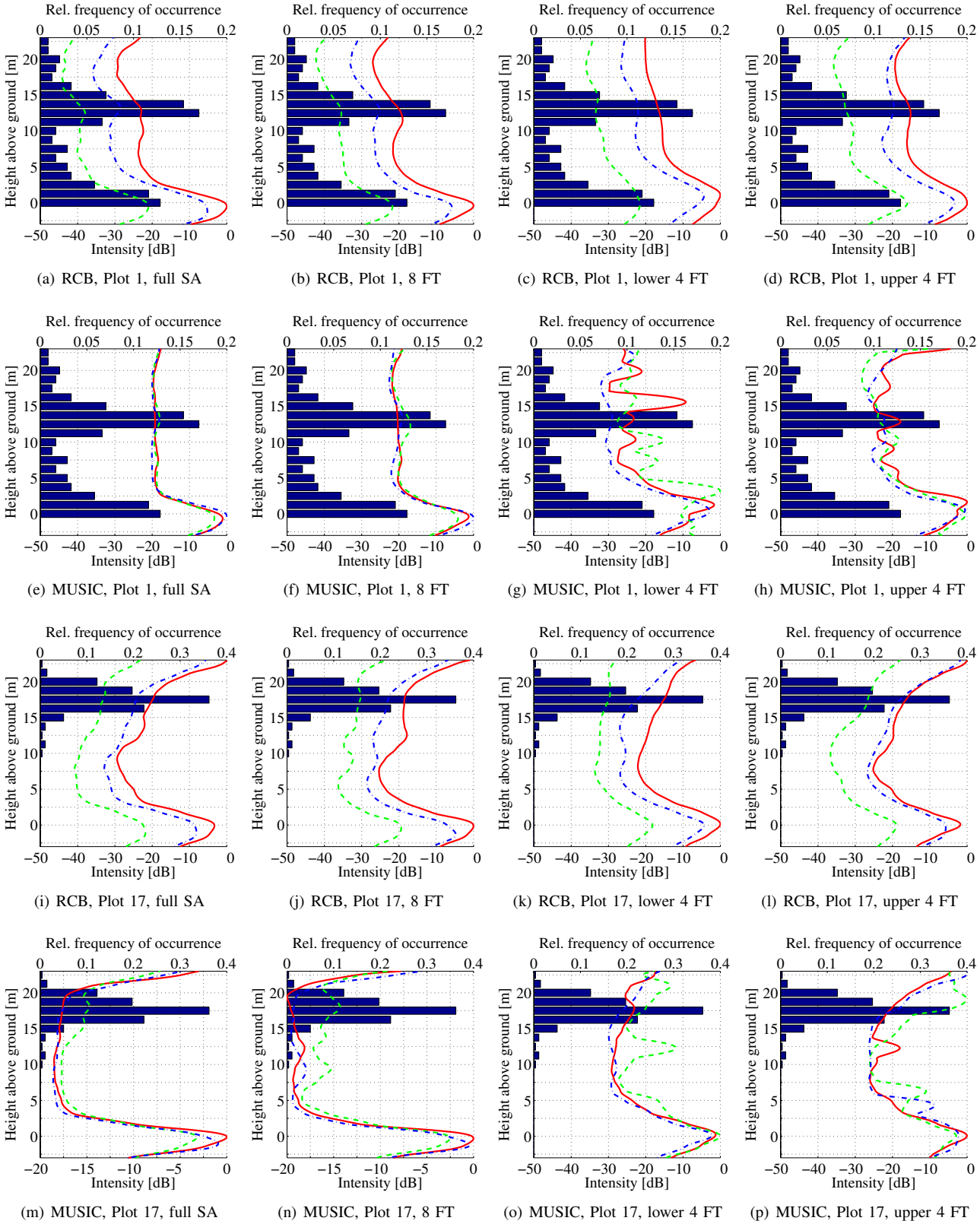

(a) RCB, Plot 1, full SA (b) RCB, Plot 1, 8 FT (c) RCB, Plot 1, lower 4 FT (d) RCB, Plot 1, upper 4 FT

(e) MUSIC, Plot 1, full SA (f) MUSIC, Plot 1, 8 FT (g) MUSIC, Plot 1, lower 4 FT (h) MUSIC, Plot 1, upper 4 FT

(i) RCB, Plot 17, full SA (j) RCB, Plot 17, 8 FT (k) RCB, Plot 17, lower 4 FT (l) RCB, Plot 17, upper 4 FT

(m) MUSIC, Plot 17, full SA (n) MUSIC, Plot 17, 8 FT (o) MUSIC, Plot 17, lower 4 FT (p) MUSIC, Plot 17, upper 4 FT

Fig. 2. Vertical profiles of relative intensities from P-band tomographic data of a forest (Plot 1, and 17) averaged over a circular sample plot of 300m^2 for the polarimetric channels HH (—), HV (– –), and VV (·–), RCB, and MUSIC. In each row, the following sequence of number of flight tracks (FT) is given, from left to right: (1) full SA (11 FT), (2) approx. half the SA (6 FT), (3) the lower 4 flight tracks, and (4) the upper 4 flight tracks. For comparison, histograms of height differences between the ALS DSM and the ALS DEM are underlaid as an external estimate of the distribution of tree heights.

tomographic focusing methods used is given in [12]. For the current analysis, only the two focusing methods robust Capon beamforming (RCB) and multiple signal classification (MUSIC) are applied, since they both provide imaging capabilities beyond Fourier resolution. The unambiguous tomographic imaging is limited to 30m in the direction perpendicular to the average line of sight. Histograms of height differences obtained from airborne laser scanning derived DSM/DEM data are used as an estimate of the distribution of tree heights.

III. Results

In Figs. 1 & 2, plots of vertical profiles of intensities are shown for the channels HH, HV, and VV, for both frequencies, L- and P-bands, and using the focusing methods robust Capon beamforming and MUSIC beamforming, respectively. Each row contains, from left to right, the following sequence of number of flight tracks (FT) used in tomographic focusing: (1) full synthetic aperture (L-band: 16 FT, P-band: 11 FT), (2) approx. half the synthetic aperture (L-band: 8 FT, P-band: 6 FT), (3) the lower four flight tracks, and (4) the upper four flight tracks (see [13], Fig. 1 for a detailed description of the acquisition geometry).

IV. Discussion

At L- and P-bands, the vertical profiles of intensities remain mostly stable for case (2), i.e., when only approx. half of the total number of flight tracks (L-band: 8 FT, P-band: 6 FT) are used for tomographic focusing. This observation is true for both focusing methods, RCB and MUSIC. When reducing the number of observations to four flight tracks, a different picture is obtained for both, the two frequencies and the different focusing methods: At L-band, the MUSIC algorithm yields corrupted estimates of vertical profiles of intensities for case (3) and (4). This observation is in line with the findings by Nannini *et al.* [7], where a required minimal number of 8 flight tracks was reported in the context of the MUSIC beamforming algorithm for a similar tomographic data set at L-band, taken over a central European forest. In general, it appears that RCB is less susceptible to a reduction of samples used. Since MUSIC is a subspace method, relying on the separation of signal and noise space, a total number of only four flight tracks does not provide an adequate number of samples in cases of distributed scatterers, or if several backscattering sources occur within a range resolution cell. The degradation is less pronounced at P-band, presumably, due to the lower number of scattering sources present at that frequency.

Besides being used for showing the potential changes in the location and intensity of measured backscattering as a function of the number of baselines, the two smallest subapertures (4 flight tracks) consisting of the outermost flight tracks are also used to indicate whether a change of the mean incidence angle of a tomographic acquisition is reflected in the vertical profiles of intensities. Since for MUSIC beamforming a considerable degradation is observed, only the RCB-based results are taken into account, here. In general, the vertical profiles of intensities show a high similarity; notable differences are only found for L-band and Plot 17, where a weaker signal is observed at ground level in case (4), and for P-band, where a lower incidence angle leads to a slightly more pronounced signal at ground level. This outcome is of somewhat limited validity as the difference in mean incidence angle between case (3) and case (4) is only 4 and 8 degrees for the L-band and the P-band case, respectively.

Acknowledgment

The authors would like to thank the procurement and technology center of the Swiss Federal Department of Defense (armasuisse W+T), in particular P. Wellig, for supporting this work. They would also like to thank the E-SAR/F-SAR team at the Department of SAR Technology, German Aerospace Center (DLR) for their ongoing cooperation.

References

[1] A. Reigber and A. Moreira, "First demonstration of airborne SAR tomography using multibaseline L-band data," *IEEE Trans. Geosci. Remote Sens.*, vol. 38, no. 5, pp. 2142–2152, 2000.

[2] F. Lombardini and A. Reigber, "Adaptive spectral estimation for multibaseline SAR tomography with airborne L-band data," in *Proc. IEEE Int. Geosci. Remote Sens. Symp.*, vol. 3, 2003, pp. 2014–2016.

[3] A. Reigber, M. Neumann, S. Guillaso, S. Sauer, and L. Ferro-Famil, "Evaluating PolInSAR parameter estimation using tomographic imaging results," in *Proc. European Radar Conf.*, 2005, pp. 189–192.

[4] M. Nannini and R. Scheiber, "A time domain beamforming algorithm for SAR tomography," in *Proc. EUSAR*, 2006, pp. 1–4.

[5] O. Frey, F. Morsdorf, and E. Meier, "Tomographic processing of multi-baseline P-band SAR data for imaging of a forested area," in *Proc. IEEE Int. Geosci. Remote Sens. Symp.*, 2007, pp. 156–159.

[6] O. Frey, F. Morsdorf, and E. Meier, "Tomographic Imaging of a Forested Area By Airborne Multi-Baseline P-Band SAR," *Sensors, Special Issue on Synthetic Aperture Radar*, vol. 8, no. 9, pp. 5884–5896, sep 2008.

[7] M. Nannini, R. Scheiber, and A. Moreira, "Estimation of the minimum number of tracks for SAR tomography," *IEEE Trans. Geosci. Remote Sens.*, vol. 47, no. 2, pp. 531–543, Feb. 2009.

[8] S. Tebaldini, "Algebraic synthesis of forest scenarios from multibaseline PolInSAR data," *IEEE Trans. Geosci. Remote Sens.*, vol. 47, no. 12, pp. 4132–4142, Dec. 2009.

[9] F. Lombardini, F. Cai, and M. Pardini, "Tomographic analyses of non-stationary volumetric scattering," in *Proc. EUSAR*, June 2010, pp. 1–4.

[10] Y. Huang, L. Ferro-Famil, and A. Reigber, "Under foliage object imaging using SAR tomography and polarimetric spectral estimators," in *Proc. EUSAR*, June 2010, pp. 1–4.

[11] S. Tebaldini, "Single and multipolarimetric SAR tomography of forested areas: A parametric approach," *IEEE Trans. Geosci. Remote Sens.*, vol. 48, no. 5, pp. 2375–2387, May 2010.

[12] O. Frey and E. Meier, "3-D time-domain SAR imaging of a forest using airborne multibaseline data at L- and P-bands," *IEEE Trans. Geosci. Remote Sens.*, vol. PP, no. 99, pp. 1–5, 2011, early access, published online.

[13] O. Frey and E. Meier, "Analyzing tomographic SAR data of a forest with respect to frequency, polarization, and focusing technique," *IEEE Trans. Geosci. Remote Sens.*, vol. PP, no. 99, pp. 1–12, 2011, early access, published online.